Spatial Consequences of Electromagnetically Induced Transparency: Observation of Electromagnetically Induced Focusing

Richard R. Moseley, Sara Shepherd, David J. Fulton, Bruce D. Sinclair, and Malcolm H. Dunn

J. F. Allen Physics Research Laboratories, Department of Physics and Astronomy, University of St. Andrews, St. Andrews, Fife KY16 9SS, Scotland

(Received 28 June 1994)

Within an experiment to produce electromagnetically induced transparency the radial intensity profile of the strong coupling laser can generate a significant spatial refractive index profile which is experienced by the weak probe laser as it tunes through the transparency window. This can lead to focusing and defocusing at separate, but close, probe laser detunings. This behavior is observed using continuous-wave lasers in rubidium vapor, in agreement with our predictions.

PACS numbers: 42.50.Gy, 42.25.Bs , 42.50.Hz, 42.60.Jf

Currently there is a wide interest in electromagnetically induced transparency (EIT) [1], both for the basic physics involved [2,3] and the enhancement of second and third order nonlinear processes [4–7]. The related topics of lasing without inversion due to atomic coherence [8,9] and the generation of a large index of refraction without absorption ("phasonium") [10,11] are also the focus of widespread study, both in theory and, recently, experiment. In this Letter we report, for the first time, what we believe to be the observation of a lens induced in the medium at the probe laser frequency by the presence of radiation from the coupling laser in an EIT arrangement. The mechanism for this lensing is the spatial profile of the strong coupling laser beam which leads to a radial refractive index variation experienced by the probe wave. This radial index profile changes with the probe laser tuning, and the probe radiation can experience both defocusing and focusing at separate frequency detuning points across the EIT window. We dub this effect "electromagnetically induced focusing" to distinguish it from self-focusing and related phenomena.

We note that control of the path of one propagating beam by another has been demonstrated by Tam and Happer [12] via an optical pumping mechanism. However, in our work the control is mediated by the EIT conditions altering the atomic susceptibilities produced in the vapor. As such, the effect is essentially nondissipative in terms of the coupling radiation, since large scale population transfers are not involved. Further, unlike self-focusing effects [13,14], there is the potential using this mechanism for focusing, trapping, and defocusing *without accompanying absorption* on the weak probe radiation.

The system considered in this work is a cascade three-level atomic scheme in rubidium as shown in Fig. 1. The rubidium system was chosen because of the close coincidence in resonant transition wavelengths for the two linked transitions: $5S$-$5P_{3/2}$ (780 nm) and $5P_{3/2}$-$5D$ (776 nm). Thus a counterpropagating experimental geometry can be used allowing transparency to be observed even when the ac Stark splitting produced by the coupling laser is less than the Doppler width of the absorption feature. Both input radiation fields were created by continuous-wave, single-frequency titanium-sapphire lasers (Microlase MBR-110, Schwartz Electro-Optic Titan-cw) pumped by separate mainframe argon-ion lasers. The probe wave was attenuated via neutral density filters to approximately 300 μW to avoid saturation and self-focusing effects, which were observed for higher powers, while the coupling laser provided 700 mW. Both lasers were focused into the 10 cm long rubidium cell from opposite ends, the coupling (probe) laser by a 50 cm (40 cm) lens giving a waist of 130 μm (80 μm) at the oven center. This focusing arrangement was chosen to give confocal parameters roughly equal to the cell length, and to ensure that the probe interacted with a significant proportion of the coupling wave spatial profile. The cell was heated to various temperatures between room temperature and 70 °C which allowed absorption lengths of the probe field at resonance, in the absence of the coupling laser, to be varied from being in excess of the

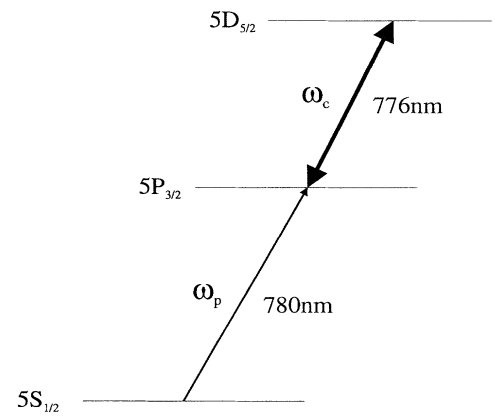

FIG. 1. A partial energy diagram of rubidium showing the level scheme used in the experiment. The lower transition ω_p is the probed in the presence of strong coupling radiation resonant with the upper transition, ω_c.

 0031-9007/95/74(5)/670(4)$06.00

cell length to some fraction of the cell length. Both polarizations were linear and horizontal.

A typical result for the transmission of the probe laser is shown in Fig. 2. Here the sharp transmission windows of EIT within each Doppler broadened absorption curve experienced by the probe laser can be clearly seen. Care was taken to ensure that this reduction in absorption was not due to some velocity-selected optical pumping mechanism. This possibility was ruled out as copropagating experiments showed no detectable reduction in absorption and varying the probe laser power had no effect on the width or depth of the EIT feature observed in the counterpropagating experiments. The limit of some 70% reduction in absorption realized by EIT in these experiments is thought to be set by the combination of two effects. First, the rubidium atomic scheme has associated hyperfine and fine structure leading to a mix of Rabi frequencies and induced splittings. Second, the induced lensing can lead to a distortion of the probe beam's propagational behavior and may diverge it outside the coupling laser mode.

In order to elucidate the induced lensing behavior, numerical calculations of the refractive index over the transparency region are required. A cascade three-level atom of the form of Fig. 1 was used as the template for a density matrix calculation of the steady-state behavior of the system. Doppler broadening was included via a numerical integration over the Maxwellian velocity distribution, with the wave vectors taken in opposite sense to allow for the counterpropagating experimental setup. An upper laser Rabi frequency of 300 MHz at the coupling beam center was used in these calculations, which matches the maximum splitting observed in the experiment. Figure 3 shows the calculated refractive index variation as the probe laser is tuned across the EIT feature for the center of the coupling laser Gaussian mode and at the $1/e^2$ point at the beam edge. The Autler-Townes splitting is less at the edge due to the

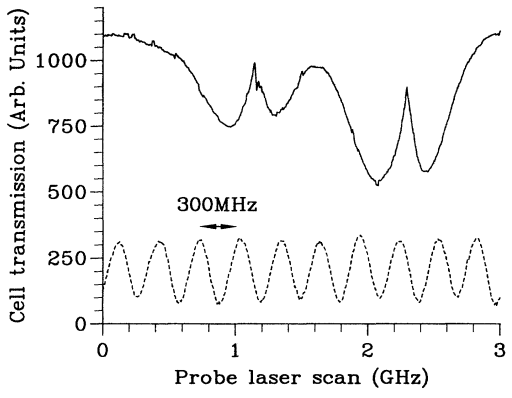

FIG. 2. Experimental transmission through the rubidium cell for a probe laser scan across the ^{87}Rb $5S_{1/2}(F = 2)$ and ^{85}Rb $5S_{1/2}(F = 3)$ to $5P_{3/2}$ transitions. (Vapor temperature ≈43 °C.)

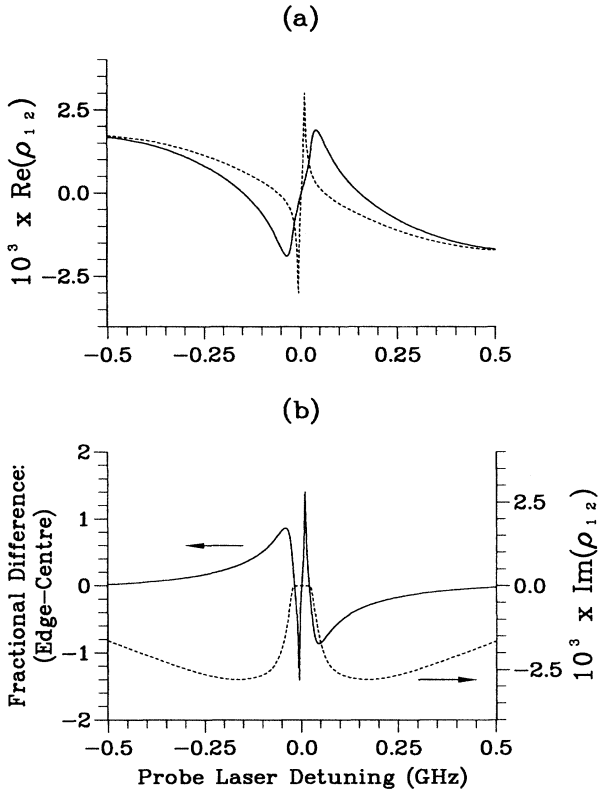

FIG. 3. (a) The real part of the off-diagonal density matrix element, which is proportional to the refractive index variation about resonance, for an upper laser Rabi frequency of (solid line) 300 MHz and (dashed line) 120 MHz. (b) A guide to the lensing action produced: the difference between the two curves in (a), normalized to the maximum deviation in refractive index as depicted by the solid line in that figure. Shown dotted (against the right-hand vertical axis) is the imaginary part of the off-diagonal density matrix element, which is proportional to the absorption on the probe laser. (Probe laser Rabi frequency 2 MHz, Doppler averaged for 40 °C.)

Gaussian beam intensity cross section and this leads to a pronounced difference between the refractive index variation experienced at the edge to that at the center of the probe beam. Figure 3(b) shows explicitly the induced focusing that we calculate will occur due to this radial modulation of the index by plotting the normalized difference between these two curves. (The absorption curve is shown as a dotted line in this plot to show the relative detuning positions of the transparency and the various lensing regions.) As the probe laser approaches in tuning from the low frequency side of the EIT feature it is initially defocused. As it tunes through the transparency window it will progressively focus and then rapidly defocus, crossing through a point of neutral lensing behavior at the two-photon resonance point. Thereafter, it will return to a focused condition which gradually fades to the high-frequency side of the transmission window.

Reference to Fig. 3(b) shows that there is sufficient radial variation in the refractive index to produce significant focusing. As shown in the figure the radial variation is of similar magnitude to the maximum deviation in refractive index from unity. We recall that the maximum magnitude of the real part of the linear susceptibility is half that of the maximum magnitude of the imaginary part, and that the absorption in the absence of the coupling laser under typical experimental conditions corresponds to an optical depth of significantly greater than one absorption length. Therefore, the induced phase difference between the probe wave front at the center and edge of the pump beam is in the order of π, and, hence, significant lensing action is expected.

Experimentally, the behavior of the probe beam upon transmission through the cell was recorded by a charge-coupled-device (CCD) array, placed about 55 cm after the cell center. As the probe laser was tuned the variations in the probe beam profile were recorded and analyzed. To associate each image of the beam with the appropriate point across the EIT feature the total probe power transmitted was determined by numerical integration over each recorded image. The results are plotted in Fig. 4(a). Individual frames are separated by approximately 1.4 MHz tuning of the probe laser, so the 80 frame sequence corresponds to a total probe frequency tuning of $\approx$110 MHz. The cell temperature was raised to 68 °C during this run so the probe intensity outside the EIT feature was essentially zero. As can be seen the frames analyzed span the maximum transparency and show a more gentle rise in transmission on the low-frequency side, which is due to a slight offset in the coupling laser tuning from exact resonance. Spatial characteristics of the probe beam after passage through the rubidium cell were characterized by determining the beam waists (width to $1/e^2$ points) at the camera. Ten frames were then analyzed. A Gaussian distribution was assumed, which was a close approximation for all the traces, except those at 42 and 56 MHz which showed some structure. Figures 4(b) and 4(c) show the variation of the probe beam waist in the horizontal and vertical dimension, respectively, as the probe laser is tuned through the EIT feature. Waist dimensions have been normalized to the beam waists observed at the camera in the absence of EIT effects. The focusing and defocusing behavior during the transparency region can be clearly seen. As predicted in the calculations above, focusing on the low-frequency side (the first frame recorded is already well into the transparency window) is followed by the sudden defocusing. Thereafter, the size reduces again on the high-frequency edge of the transparency. The maximum transparency occurs at a point of neutral focusing but not on the focused to defocused crossing as predicted above.

We note that self-focusing has been considered in the context of EIT systems by Rathe *et al.* [15] arising through the dependence of the third-order susceptibility on the field of the probe laser. However, we emphasize that the effect described here is not a self-induced one, but is rather the modification of one beam (probe) by another (coupling). This was verified by using a lower vapor temperature, so that the probe was not completely attenuated outside the transparency region, under which conditions probe beam size changes were only seen during the transparency region. Furthermore, reducing the probe power did not lead to any reduction in the lensing

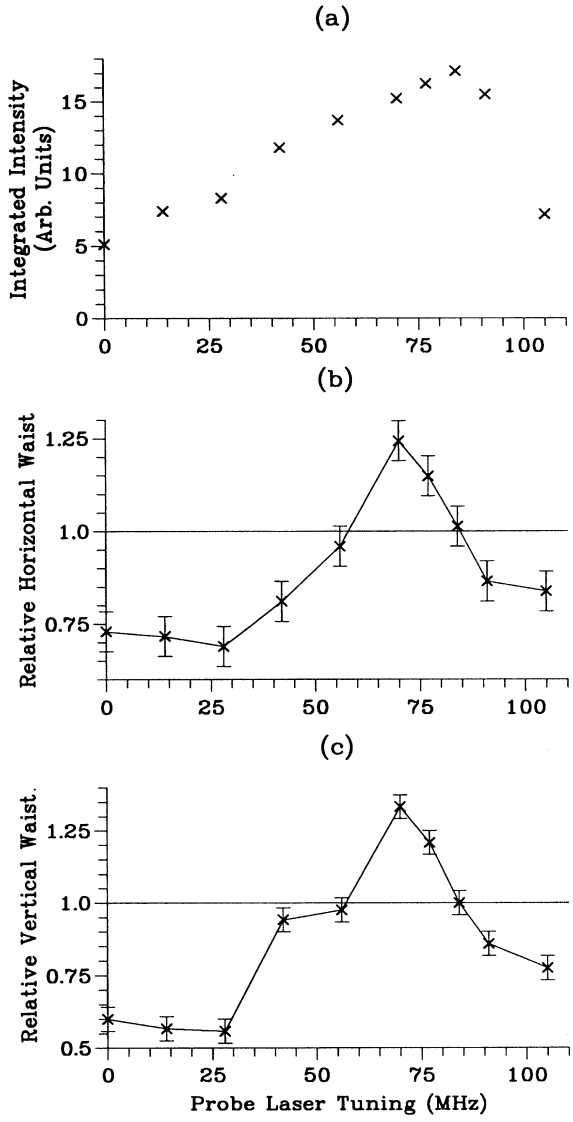

FIG. 4. Integrated intensity (a), and below, horizontal (b) and vertical (c) waists, normalized to the off-resonance probe waist, for selected images of the probe during the transparency. The narrow probe tuning region covers the peak of the EIT window. [Vapor temperature 68 °C, ^{85}Rb : $5S_{1/2}(F = 3) \rightarrow 5P_{3/2}$ transition.]

effects, as would have been expected if this had been a self-induced phenomena. We also verified that higher temperatures lead to greater lensing action as expected.

Electromagnetically induced focusing has critical implications for future experiments in the area of atomic coherence effects. Mode matching of coupling laser and the circulating laser mode in inversionless lasers will be affected, as will all EIT experiments, including the enhancement of nonlinear processes. Of particular interest will be the susceptibility to this lensing of the various schemes for enhanced refractive index without absorption. The probe laser will be subject to very strong lensing at the point of minimum absorption and maximum refraction. We note, however, that at the line center of EIT the probe laser should not experience any focusing or defocusing but stress that the frequency bandwidth for this neutral zone is very tight, as shown in Fig. 3. Experiments designed to avoid lensing may utilize either a "top-hat" coupling laser mode, or ensure that the probe is contained in a sufficiently small area of the strong laser to avoid a spatial variation in refractive index.

In addition to the change in spot size observed, we have also observed beam deflection due to nonperfectly overlapped lasers and filamentation of the probe laser into two components. Detailed calculations, taking into account the changing spatial conditions within the cell are left for further work. Foremost in future experimental prospects is the demonstration of the range of lensing possible all within the transparent flat top of the EIT feature, as predicted in Fig. 3. Within this region electromagnetically induced focusing should be able to provide a lens controllable via one laser on another in a nondissipative situation over a wide range of focal lengths.

To summarize the main points of this Letter: We have studied EIT using counter-propagating continuous-wave lasers and shown how the radial variation of the strong coupling laser radiation may lead to electromagnetically induced focusing and defocusing of the weak probe laser. Both focusing and defocusing were observed experimentally and this phenomena has important implications for the design of future experiments in this area, and is interesting in its own right as a variable lens induced on one laser beam by another, without high associated absorption on either wave.

We acknowledge financial support from the Science and Engineering Research Council and one of us (R. M.) also thanks the Carnegie Trust for the Universities of Scotland for personal support.

[1] K.-J. Boller, A. Imamoğlu, and S. E. Harris, Phys. Rev. Lett. **66**, 2593 (1991).
[2] S. E. Harris, Phys. Rev. Lett. **70**, 552 (1993).
[3] J. Eberly, M. L. Pons, and H. R. Haq, Phys. Rev. Lett. **72**, 56 (1994).
[4] S. E. Harris, J. E. Field, and A. Imamoğlu, Phys. Rev. Lett. **64**, 1107 (1990).
[5] K. Hakuta, L. Marmet, and B. P. Stoicheff, Phys. Rev. Lett. **66**, 596 (1991); Phys Rev A **45**, 5152 (1992).
[6] G. Z. Zhang, K. Hakuta, and B. P. Stoicheff, Phys. Rev. Lett. **71**, 3099 (1993).
[7] R. R. Moseley, B. D. Sinclair, and M. H. Dunn, Opt. Commun. **101**, 139 (1993).
[8] A. Imamoğlu, J. E. Field, and S. E. Harris, Phys. Rev. Lett. **66**, 1154 (1991).
[9] O. Kocharovskaya, Phys. Rep. **219**, 175 (1992).
[10] M. O. Scully and S.-Y. Zhu, Opt. Commun. **87**, 134 (1992).
[11] M. O. Scully, Phys. Rep. **219**, 191 (1992).
[12] A. C. Tam and W. Happer, Phys. Rev. Lett. **38**, 278 (1977).
[13] A. Javan and P. L. Kelley, IEEE J. Quantum Electron. **QE-2**, 470 (1966).
[14] J. E. Bjorkholm and A. Ashkin, Phys. Rev. Lett. **32**, 129 (1974).
[15] U. Rathe *et al.*, Phys. Rev. A **47**, 4994 (1993).